Macromolecules

Article

pubs.acs.org/Macromolecules

Yielding Behavior of Tough Semicrystalline Hydrogels

Cigdem Bilici,[†] Semra Ide,[‡,§] and Oguz Okay*[,†]

[†]Department of Chemistry, Istanbul Technical University, 34469 Maslak, Istanbul, Turkey

[‡]Department of Physics Engineering and [§]Department of Nanotechnology and Nanomedicine, Hacettepe University, 06800 Beytepe, Ankara, Turkey

Supporting Information

ABSTRACT: Supramolecular semicrystalline hydrogels are soft functional materials consisting of water-swollen hydrophilic polymer chains interconnected by hydrophobic segments forming lamellar crystals. Although such hydrogels with high crystallinity are mechanically strong, with elastic moduli and tensile strength of 80−300 MPa and 4−7 MPa, respectively, they are brittle and rupture at a stretch of less than 20% without yielding. Here, we report that the incorporation of a small amount of a weak hydrophobe into semicrystalline hydrogels significantly increases their toughness and stretchability without losing their high modulus and high strength. We design a highly entangled physical network based on poly(*N*,*N*-dimethylacrylamide) (PDMA) chains containing *n*-octadecyl acrylate (C18A) and lauryl methacrylate (C12M) segments with side chain lengths of 18 and 12 carbons, respectively. By including 0.1−0.4 mol % C12M into the PDMA backbone containing 30 mol % C18A segments, we were able to create more ordered and thinner lamellar crystals with a layered structure. Simultaneously, a brittle-to-ductile transition was observed due to the appearance of necking behavior leading to 10-fold increase of toughness. The significant toughness improvement upon incorporation of C12M into the semicrystalline hydrogels could be explained with the appearance of active tie molecules under external force interconnecting the lamellar clusters. The hydrogels also exhibit reversible tensile deformation induced by heating above the melting temperature of crystalline domains.

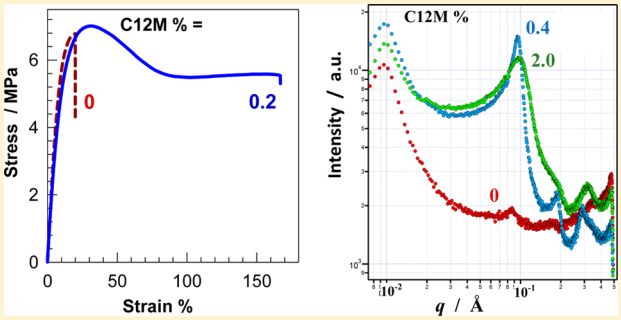

INTRODUCTION

Hydrogels are unique soft materials with similarity to biological tissues and therefore attracted great interest for a wide range of application areas.[1,2] A significant achievement in the preparation of new generation hydrogels with extraordinary mechanical properties is the double-networking strategy developed by Gong and co-workers.[3−5] Double-network (DN) hydrogels consist of interpenetrated and interconnected polymer network components containing 60−90% water.[3−7] The highly cross-linked first-network consists of stretched network chains and therefore it is brittle in nature, while the loosely cross-linked second-network forming the major component of the DN exhibits viscoelastic and ductile behavior.

The deformation of DNs possessing a high toughness usually proceeds via a yield phenomenon which is macroscopically evidenced by the appearance of necking.[8−10] Figure 1a schematically illustrates typical mechanical behavior of a DN hydrogel subjected to two successive tensile tests before fracture. The virgin DN shows a distinct yield point where the brittle first network starts to break up to form many cracks while the second ductile network keeps the macroscopic sample together, leading to excellent toughness.[10] However, breaking chemical bonds in the first network during the first loading results in an irreversible damage to the DN, as evidenced from the significant decrease of both the modulus and the toughness during the second loading (Figure 1a). This is the main disadvantage of DN hydrogels. To overcome this weakness, hybrid DNs have recently been synthesized consisting of physically and chemically cross-linked network components.[11−13] However, their fracture stresses are low as compared to the classical DNs due to the presence of noncovalent cross-links.

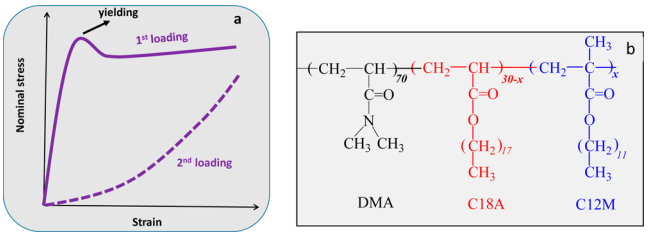

Figure 1. (a) Scheme of stress−strain curves of a tough DN hydrogel in the first (solid curve) and second tensile loading before fracture (dashed curve). (b) Structure of the monomer units of the hydrogels.

Because the DN synthesis is lengthy and complicated, a simple one-pot synthesis of such mechanically strong soft materials would be attractive for many applications. Moreover,

Received: March 8, 2017
Revised: April 17, 2017
Published: April 20, 2017

DOI: 10.1021/acs.macromol.7b00507
Macromolecules 2017, 50, 3647−3654

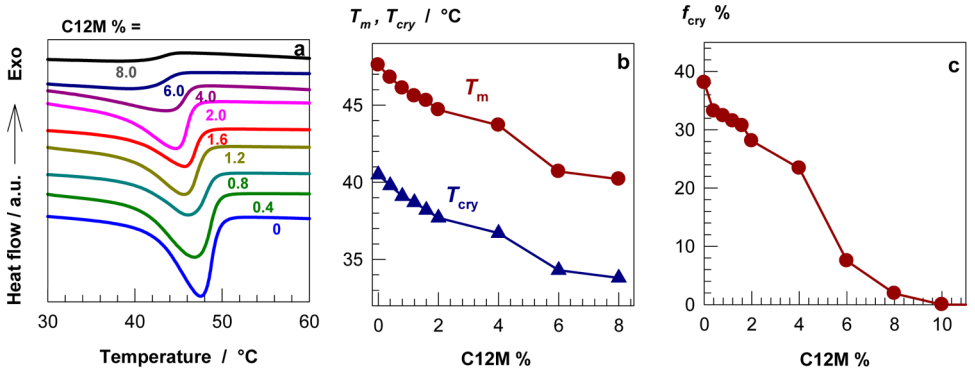

Figure 2. (a) DSC traces of the hydrogels with various C12M contents. (b) Melting T_m and crystallization temperatures T_{cry} of the hydrogels plotted against C12M %. (c) The fraction f_{cry} of C18A segments in crystalline domains (moles of crystallized C18A/mole of C18A) calculated from the area under the melting peaks plotted against C12M %.

in contrast to the irreversible deformation of the DNs, reversible tensile deformation at both prenecking and necking regimes is also required to create self-healing ability in such hydrogels. Recently, Gong et al. prepared polyampholyte single-network hydrogels of high toughness consisting of strong and weak physical bonds at high concentrations,[14] while Hu et al. designed hybrid hydrogel systems formed via strong covalent bonds and clusters of hydrogel bonds.[15] Another group of high-strength single-network hydrogels is the semicrystalline hydrogels consisting of hydrophilic polymer chains interconnected by hydrophobic segments with long side alkyl chains such as *n*-alkyl(meth)acrylates forming lamellar crystals.[16−18] Osada was the first to prepare such hydrogels based on chemically cross-linked poly(acrylic acid) network chains containing hydrophobic domains.[16] Recently, supramolecular semicrystalline hydrogels with self-healing and shape-memory functions have been prepared via micellar and bulk polymerization techniques.[19−21] It was shown that although the hydrogels with high crystallinity are mechanically strong, with elastic moduli and tensile strength of 80−300 MPa and 4−7 MPa, respectively, they are brittle and rupture at a stretch of less than 20% without yielding.[21] The challenge of producing stretchable and tough semicrystalline hydrogels of high mechanical strength is thus inherent.

Here, we report that the incorporation of a small amount of a weak hydrophobe into semicrystalline hydrogels significantly increases their toughness and stretchability without losing their high modulus and high strength. We design a highly entangled physical network formed via lamellar crystals consisting of aligned side alkyl chains. The network bases on poly(*N*,*N*-dimethylacrylamide) (PDMA), which is a very useful hydrophilic biocompatible polymer with associative properties (Figure 1b).[22−24] The interconnected lamellar crystals forming a layered hydrogel structure are created by incorporating *n*-octadecyl acrylate (C18A) and lauryl methacrylate (C12M) segments with side chain lengths of 18 and 12 carbons, respectively, into the PDMA backbone (Figure 1b). As reported before, hexagonal packing of side alkyl chains of C18A segments create alkyl crystals in the hydrogels,[16−19] while C12M segments with shorter side alkyl chains and α-methyl groups contribute to the hydrophobic associations.[25−27] As will be seen below, by including 0.1−0.4 mol % C12M into the polymer backbone consisting of 70 mol % DMA and 30 mol % C18A segments, we were able to generate more ordered and thinner lamellar crystals with a layered structure. Simultaneously, a brittle-to-ductile transition was observed due to the appearance of necking behavior leading to 10-fold increase of toughness. The significant toughness improvement upon incorporation of C12M into the semicrystalline hydrogels could be explained with the appearance of active tie molecules under external force interconnecting the lamellar clusters. The hydrogels also exhibit reversible tensile deformation induced by heating above the melting temperature of crystalline domains.

RESULTS AND DISCUSSION

Characteristics of the Hydrogels. The hydrogels were prepared by bulk photopolymerization of DMA, C18A, and C12M in the presence of Irgacure 2959 as the photoinitiator at a concentration of 0.1 wt %. The monomers and the initiator were first mixed to obtain a homogeneous solution, and then the polymerization was conducted at 23 ± 2 °C for 1 day under UV lamp at a wavelength of 360 nm (for details, see the Supporting Information). The total amount of the hydrophobic monomers C18A and C12M in the comonomer feed was fixed at 30 mol % while the amount of C12M was varied between 0 and 20 mol %. In the following, the C12M content of the hydrogels is denoted by C12M %, which represents the mole percent of C12M in the comonomer feed. For instance, the hydrogel with 0.1% C12M was prepared from a comonomer feed consisting of 70 mol % DMA, 29.9 mol % C18A, and 0.1 mol % C12M. Preliminary experiments showed that a reaction time of 1 day was needed for the complete conversion of the monomers to the water-insoluble copolymer (Figure S1). After equilibrium swelling of the terpolymers in water, the water content of the hydrogels was between 26 and 37 wt % that increased with increasing C12M content (Figure S1). The increase in the water content is attributed to the decreasing crystallinity of the hydrogels upon increasing C12M % (see below).

The hydrogels equilibrium swollen in water contained crystalline domains as evidenced by DSC, SAXS, WAXS, and rheological measurements. DSC scans of the hydrogels with ≤8% C12M showed melting and crystallization peaks while the peaks disappeared at higher C12M contents (Figure 2a and Figure S2). Figure 2b shows the melting T_m and crystallization temperatures T_{cry} of the hydrogels plotted against their C12M contents. T_m and T_{cry} are between 40−48 and 34−40 °C, respectively, and they decrease upon increasing C12M %, indicating decreasing thermal stability of alkyl crystals in the hydrogels. This is expected as the added C12M segments do not contribute to the formation of alkyl crystals because of its short alkyl side chain.[25,26] In Figure 2c, the fraction f_{cry} of C18A

DOI: 10.1021/acs.macromol.7b00507
Macromolecules 2017, 50, 3647−3654

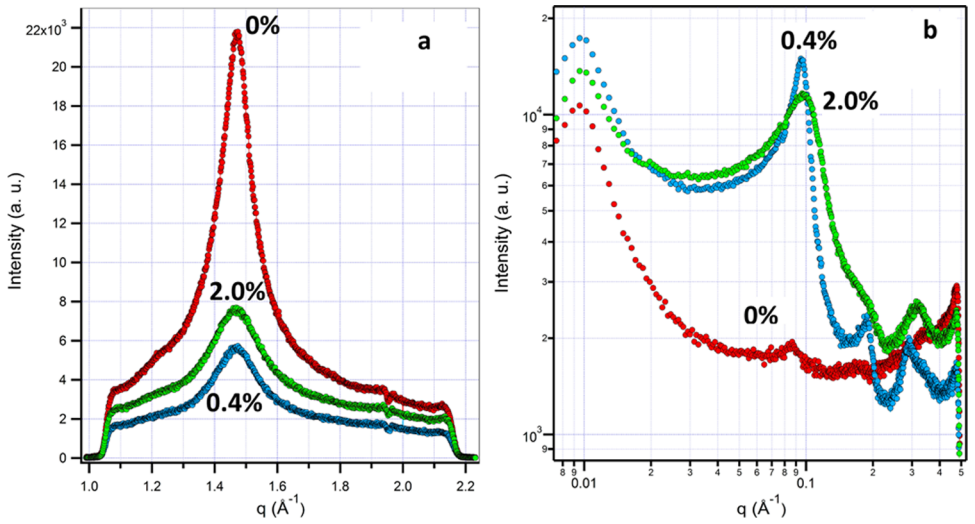

Figure 3. WAXS (a) and SAXS profiles (b) of the hydrogel samples without and with 0.4 and 2% C12M where the scattering intensity $I(q)$ is plotted against the scattering vector q. C12M contents are indicated.

segments in crystalline domains (moles of crystallized C18A/mole of C18A) calculated from the area under the melting peaks are plotted against C12M %. The maximum degree of crystallinity observed in the absence of C12M is 38%, indicating that 38% of C18A segments form alkyl crystals while the remaining part contributes to the hydrophobic associations.[27,28] The crystallinity decreases with increasing C12M %, and no crystalline domains exist above 8% C12M. Thus, the relative content of the crystalline and noncrystalline domains can be adjusted by varying C12M content in the monomer feed.

Figure 3a shows wide-angle X-ray scattering (WAXS) profiles of the hydrogels without and with 0.4 and 2% C12M where the scattering intensity $I(q)$ is plotted against the scattering vector q. Independent on the amount of C12M, WAXS data show a high intensity peak at q_{max} = 1.46 Å^{-1}, corresponding to a short-range ordering with a constant lattice spacing d_1 of 0.43 nm. This spacing was reported before for the crystalline state of both dry and swollen *n*-alkyl(meth)acrylate (co)-polymers[16−19,29−35] and indicates side-by-side packing between the octadecyl (C18) side chains in the hydrogels, as illustrated in Scheme 1. The constancy of d_1 spacing also indicate that side-by-side arrangement of alkyl chains is not affected by the incorporation of C12M segments into the polymer chains. Moreover, the peak intensity decreases and slightly broadens with the addition of C12M, which is consistent with slightly lower crystallinity of C12M-containing hydrogels (Figure 2c). This also reveals that the number of C18 chains per lamellar crystal decreases, i.e., a larger number but thinner lamellar crystals form with the incorporation of C12M segments.

Scheme 1. Cartoon Showing Crystalline and Amorphous Domains of the Hydrogels

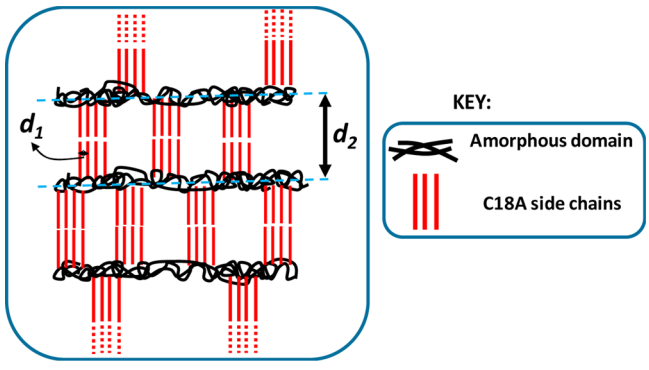

Small-angle X-ray scattering (SAXS) profiles of the hydrogels in a semilogarithmic scale are shown in Figure 3b. The hydrogels containing C12M exhibit a high intensity peak at q_{max} = 0.094 and 0.096 Å^{-1}, indicating a long-range ordering with lattice spacings d_2 of 6.7 and 6.5 nm for 0.4 and 2% C2M, respectively. The hydrogel with 0.4% C12M exhibits the sharpest peak, while without C12M this peak is weak and broad at a q_{max} = 0.086 Å^{-1} (d_2 = 7.3 nm). Higher intensity and sharpening of the SAXS peak upon addition of C12M reveal formation of thinner lamellar crystals and increasing order in the hydrogels. The d_2 spacing also reveals tail-to-tail alignment of the side chains perpendicularly to the main chain, as reported before for semicrystalline hydrogels (Scheme 1).[16−18] Because the length l_{max} of the fully extended octadecyl (C18) chain is 2.43 nm,[36,37] the d_2 spacing of the present hydrogels (6.5−7.3 nm) is larger than twice of the fully extended C18 chain length ($2l_{max}$ = 4.86 nm). The difference between d_2 and $2l_{max}$, which is between 1.6 and 2.4 nm for the present hydrogels, is attributed to the thickness of polymer backbone (amorphous domain) separating alkyl crystals (Scheme 1).[16,17] Thus, WAXS and SAXS data suggest side-by-side packing of alkyl chains in the hydrogels and formation of more ordered and thinner lamellar crystals with a layered structure after incorporation of C12M segments in the hydrogels. Moreover, the most significant change in the microstructure of the hydrogels appears upon addition of a small amount of C12M (0.4%). As will be seen in the next section, this is reflected in their mechanical properties.

Rheological measurements are another means of studying the transitions between crystalline and amorphous states depending on the temperature. Figure 4a shows temperature sweep results of the hydrogels without and with 0.4 and 2% C12M during heating from 25 to 65 °C at a heating rate of 1 °C min^{-1}. Here, the storage G' (filled symbols) and loss modulus G'' (open symbols) of the hydrogels measured at an angular frequency ω of 6.3 rad s^{-1} are plotted against the temperature. The vertical lines in the figure represent the melting temperatures of the hydrogels, which are 48, 47, and 45 °C for 0, 0.4, and 2% C12M, respectively. At 25 °C, the hydrogels exhibit a storage

DOI: 10.1021/acs.macromol.7b00507
Macromolecules 2017, 50, 3647−3654

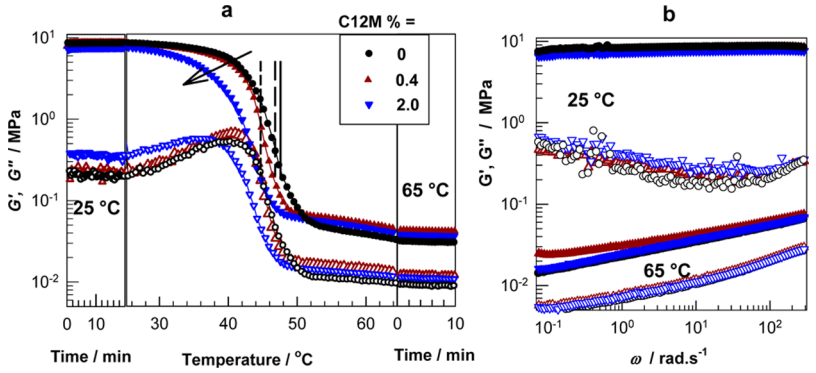

Figure 4. (a) G' (filled symbols) and G'' (open symbols) of the hydrogels during cooling and heating scans between 25 and 65 °C. The vertical lines represent the melting temperatures of the hydrogels without (solid line) and with 0.4 (long-dashed line) and 2% C12M (short-dashed line). ω = 6.3 rad s^{-1}. γ_0 = 0.001. (b) G' (filled symbols) and G'' (open symbols) of the hydrogels at below and above the melting temperature T_m plotted against the frequency ω. γ_0 = 0.001. C12M contents of the hydrogels are indicated in (a).

modulus G' of 7.6−8.3 MPa and a loss factor tan δ (= G''/G') of 0.02−0.05, while upon heating above T_m, G' decreases by more than 2 orders of magnitude and becomes 0.03−0.04 MPa at 25 °C. Simultaneously, tan δ increases to 0.3 as typical for weak gels. The strong-to-weak gel transition observed during heating is completely reversible with a slight hysteresis (Figure S3), as typically observed in semicrystalline hydrogels.[19,20] As indicated by the arrow in Figure 4a, increasing C12M content, that is, decreasing T_m, of the hydrogels shifts the strong-to-weak gel transition to lower temperatures. The frequency sweep results of the hydrogels shown in Figure 4b reveal that below T_m G' is independent of the frequency ω over the whole experimental window, while it is frequency dependent above T_m and proportional to $\omega^{-0.17\pm0.02}$ without any plateau in G' vs ω curve.

Mechanical Properties. Figure 5a compares stress−strain curves of the hydrogels prepared without (dashed curve) and

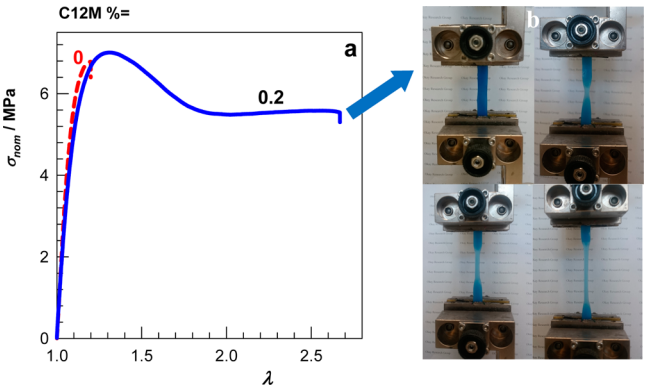

Figure 5. (a) Typical tensile stress−strain curves of the hydrogels without (red dashed curve) and with 0.2% C12M (blue solid curve) as the dependence of nominal stress σ_{nom} on the elongation ratio λ. $\dot{\varepsilon}$ = 8.3 × 10^{-2} s^{-1}. (b) Images demonstrating the necking behavior of the hydrogel with 0.2% C12M. The gel sample was colored for clarity.

with 0.2% C12M (solid curve). The stress is presented by its nominal value σ_{nom}, which is the force per cross-sectional area of the undeformed gel specimen, while the strain is given by the deformation ratio λ (deformed length/initial length). The common feature of the two hydrogels is that the initial slope of the curves, i.e., the Young's modulus E, is almost the same, 71 ± 3 and 70 ± 5 MPa for 0 and 0.4% C12M, respectively. This reveals that inclusion of such a small amount of the weak hydrophobe C12M into the polymer backbone does not affect the cross-link density of the hydrogel. However, the gel sample prepared without C12M fails in a brittle fashion at a stretch (λ − 1) of 20%, while the one with 0.2% C12M shows necking behavior, as seen in Figure 5b, leading to a 10-fold increase in toughness, calculated from the area below the stress−strain curve up to the fracture point, (from 1.0 ± 0.2 to 9.6 ± 0.3 MJ m^{-3}) and 8-fold increase in stretchability (from 20 to 167%). Thus, a brittle-to-ductile transition can be induced upon incorporation of a small amount of C12M into the polymer chains.

Tensile tests were also conducted at different strain rates $\dot{\varepsilon}$ on hydrogel samples prepared at various C12M contents. Figure 6a shows stress−strain curves of the hydrogels at a fixed strain rate $\dot{\varepsilon}$ but at various levels of C12M, while in Figures 6b1 and 6b2 the curves were obtained by varying the strain rate $\dot{\varepsilon}$ at fixed levels of C12M. Both the amount of C12M and strain rate significantly affect the mechanical behavior of the hydrogels. Between 0.1 and 2% C12M where a significant yielding appears (inset to Figure 6a), the modulus, fracture stress, and toughness only slightly decrease with increasing C12M % while they rapidly decrease above 2% C12M (Figure S4). High stretchable hydrogels with a high elongation ratio at break (up to 1600%) could be produced at high C12M contents.

The variation of the yield stress σ_y with the C12M content and strain rate $\dot{\varepsilon}$ shows several interesting features. For instance, although the hydrogel without C12M is brittle, inclusion of 0.1% C12M; i.e., 1 C12M per 1000 segments into the polymer leads to the appearance of a significant necking and the highest yield stress σ_y of 7.3 MPa. Further addition of C12M linearly decreases the yield stress σ_y according to the relation σ_y = 7.1 ± 0.1 − C12M mol % (Figure 6c). The extrapolated value of σ_y to 0% C12M is thus 7.1 MPa, which is close to the fracture stress of the brittle hydrogel prepared without C12M (6.8 ± 0.3 MPa). Because no yielding appears at 0% C12M, this suggests that in the absence of C12M, the molecular mobility between crystalline domains is insufficient to produce yielding at the time scale of the mechanical tests ($\dot{\varepsilon}$ = 8.3 × 10^{-2} s^{-1}).

At a fixed level of C12M (Figures 6b1 and 6b2), the yield stress σ_y rises with the strain rate $\dot{\varepsilon}$, and this rise is linear when plotted against the logarithm of $\dot{\varepsilon}$ (Figure 6d), in accord with the Eyring model of mechanically induced dissociation of molecular bonds[38−40]

DOI: 10.1021/acs.macromol.7b00507
Macromolecules 2017, 50, 3647−3654

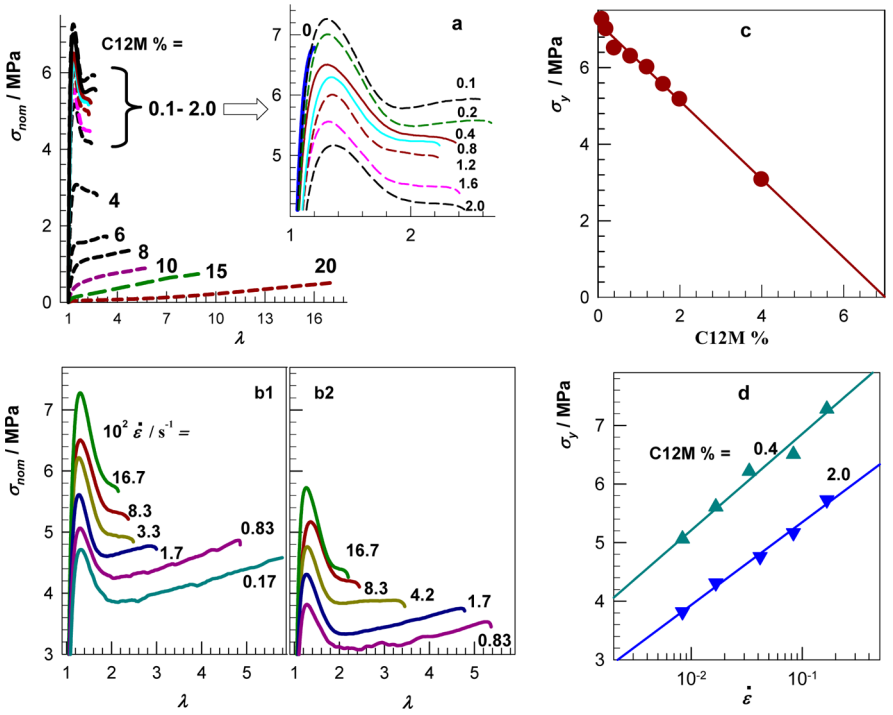

Figure 6. (a, b1, b2) Tensile stress−strain curves of the hydrogels with various C12M contents at $\dot{\varepsilon} = 8.3 \times 10^{-2}$ s^{-1} (a) and at various $\dot{\varepsilon}$ with 0.4% (b1) and 2% C12M (b2). The inset is a zoom-in to necking regime. (c, d) Yield stress σ_y plotted against C12M % (c) and the logarithm of the strain rate $\dot{\varepsilon}$ (d). The solid lines are the best fits to the data.

Scheme 2. Cartoon Presenting Two Lamellar Clusters Interconnected by Two Active Tie Molecules (a) and Deformation of Lamellar Clusters under Force (b) and Their Destroying at the Yield Point (c)[a]

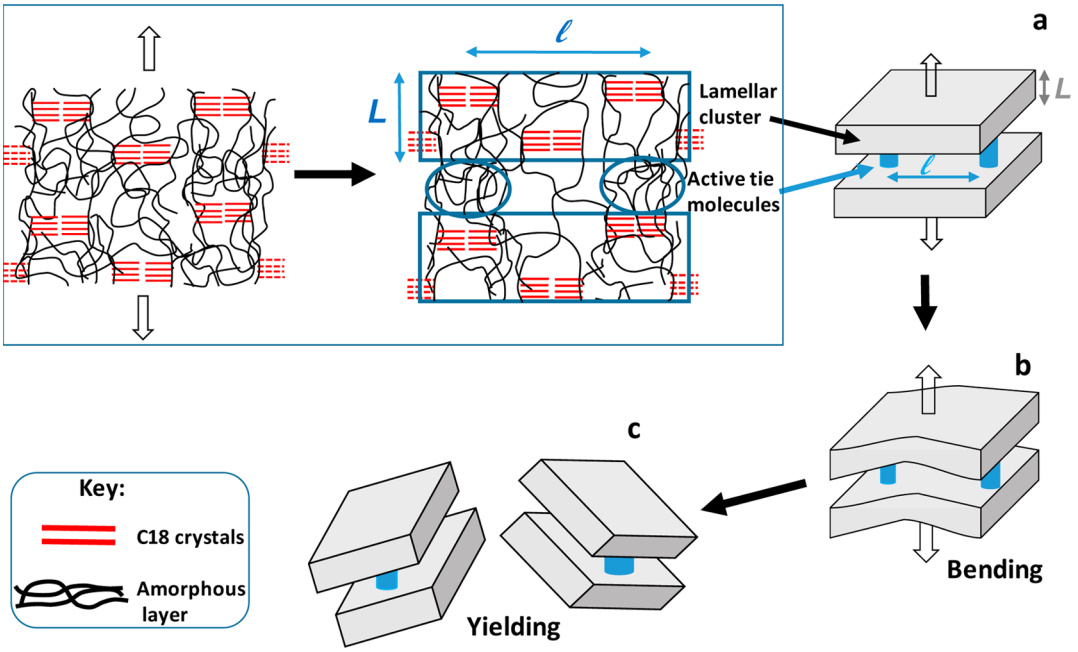

[a]In part a, rectangles and circles indicate lamellar clusters and tie molecules, respectively.

$$\sigma_y = \frac{2kT}{V_a} \ln(\dot{\varepsilon}/\varepsilon_0) + \frac{2E_a}{V_a} \quad (1)$$

where V_a is the activation volume, E_a is the activation energy, ε_0 is the pre-exponential factor, k is the Boltzmann constant, and T is the absolute temperature. The slopes of the best-fit lines to the σ_y vs ln $\dot{\varepsilon}$ data give the activation volume V_a as 11.5 ± 0.4 and 13 ± 2 nm^3 for 0.4% and 2% C12M, respectively (Figure 6d). Because V_a can be regarded as the size of the polymer segments in the hydrogels involved in the cooperative motion resulting in yielding, increasing V_a with rising C12M content indicates increasing number of mobile segments, i.e., enhanced molecular mobility between crystalline domains. Moreover, the activation energy E_a is related to the height of energy barrier to

DOI: 10.1021/acs.macromol.7b00507
Macromolecules 2017, 50, 3647−3654

overcome the mobile segments to move by the application of an external force. For the present hydrogels, this energy corresponds to the dissociation energy of hydrophobic associations, which is close to 0.98kT per methylene group of alkyl chains.[41−43] Because increasing C12M content decreases the average length of side alkyl chains, the magnitude of the energy barrier reduces so that the dissociation of physical cross-links requires a lower mechanical stress. We have to note that even the brittle hydrogel formed in the absence of C12M exhibited yielding behavior at low strain rates $\dot{\varepsilon}$. For instance, a brittle-to-ductile transition in the hydrogels prepared without C12M can also be induced by reducing the strain rate from 8.3 $\times$ 10^{-2} to 4 $\times$ 10^{-3} s^{-1} although the corresponding yield stress was significantly lower than that of C12M-containing hydrogels (Figure S5).

We can explain the significant toughness improvement in semicrystalline hydrogels upon addition of C12M with the formation of layered lamellar crystals as revealed by SAXS measurements. Previous works conducted on semicrystalline polymers indicate that the existence of so-called active tie molecules interconnecting the lamellar clusters play a significant role in their mechanical strength and yielding behavior.[44−50] For the present hydrogels, the applied external force during tensile testing results in the unfolding of the amorphous layers between lamellar crystals, leading to the appearance of lamellar clusters interconnected by tie molecules, as schematically illustrated in Scheme 2a. Lamellar clusters consist of several lamellar crystals separated by amorphous domains, and tie molecules bridging them are part of the amorphous region but they are able to unfold under the external force.

PDMA chains involved in hydrophobic associations through noncrystallized C18A and C12M segments can be considered as active tie molecules bridging the lamellar clusters. These molecules dissipate energy by transmitting the external load from one to the another lamellar cluster whereby the clusters are deformed, as illustrated in Scheme 2b. As the hydrogel sample is stretched, the stress generated from the tie molecules may reach a critical value under which the lamellar clusters are broken and fragmented, leading to the yielding phenomenon (Scheme 2c). In the absence of C12M, no yielding occurs because the lamellar clusters do not form a layered structure and the deformation of the chains between the lamellae in the direction of elongation is too slow to pass over the potential energy barrier. Thus, there are no active tie molecules in the hydrogels without C12M. Addition of C12M segments induces self-assembly of lamellar clusters to form a layered structure. Simultaneously, the magnitude of the energy barrier decreases due to weakening of lamellar crystals, and the number of interlamellar active tie molecules increases so that yielding appears. Increasing activation volume V_a with increasing C12M content also reveals the movement of larger domains during deformation of the hydrogels as the C12M content is increased.

According to the lamellar cluster model of Nitta et al.,[47−50] the bending force acting on the lamellar clusters through the tie molecules results in disintegration of the clusters into their fragments, and this occurs at the yield point. Assuming that the onset of disintegration of the lamellar cluster occurs when the elastic energy reaches a critical value U_y, the yield stress σ_y of semicrystalline polymers is given by[47−50]

$$\sigma_y = 2\sqrt{2EU_y}\,(L/l)^2 \qquad (2)$$

where L is the thickness of lamellar clusters interconnected by tie molecules with a support span length l ($l > L$, Scheme 2a). We estimated the yield energy U_y of the hydrogels from the area under the stress−strain curve up to the yield point. In Figure 7a, σ_y is plotted against $\sqrt{2EU_y}$ for the hydrogels with various C12M contents (filled symbols) and at various strain rates (open symbols). It is seen that in accord with eq 2 all the data fall onto the same line with a slope 0.46 ± 0.01. The average l/L is 2.09 ± 0.03, indicating that the distance between adjacent active tie links is about twice the thickness of the lamellar clusters (Figure 7b). $l/L \cong 2$ was also reported for semicrystalline polymers such as polyethylene and isotactic polypropylene[46,48,49] and reveals that the minimum size of fragmented clusters $L(l/2)^2$ is close to L^3. The thickness L of lamellar clusters was estimated as almost equal to the end-to-end distance of unperturbed polymer chains in the melt.[47] This means that the minimum size L^3 of fragmented clusters corresponds to the spatial dimension of a single chain. Thus, the lamellar cluster model shown schematically in Scheme 2 well explains the yielding behavior of semicrystalline hydrogels, and the lamellar clusters are fragmented into polymer chains at the yield point.

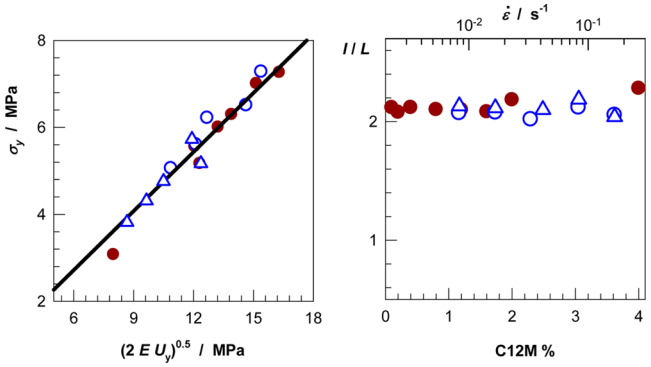

Figure 7. (a) Yield stress σ_y plotted against $\sqrt{2EU_y}$ for the hydrogels with various C12M contents at $\dot{\varepsilon}$ = 8.3 $\times$ 10^{-2} s^{-1} (filled symbols) and at various strain rates $\dot{\varepsilon}$ with 0.4% (open circles) and 2% C12M (open triangles). (b) l/L data of all hydrogels shown as a function of C12M % (filled symbols) and $\dot{\varepsilon}$ (open symbols).

Because of the supramolecular nature of the present hydrogels, fragmented lamellar clusters could be repaired by melting the alkyl crystals above T_m and subsequent cooling to room temperature. The temperature-induced recovery of the crystal structure resulted in almost reversible stress−strain curves as illustrated in Figure 8a. The solid curve in the figure presents the stress−strain curve of a virgin hydrogel sample with 0.4% C12M that is stretched to 100% elongation. The modulus E and the yield stress σ_f of the virgin hydrogel are 68 ± 2 and 6.5 ± 0.2 MPa, respectively (Figure 8b). The dotted curve in Figure 8a presents the stress−strain curve of the same hydrogel sample subjecting to a second tensile test up to 110% elongation. The modulus drastically decreases to 5.3 ± 0.1 MPa, and the yielding peak disappears, indicating the damage created in the lamellar clusters. This behavior is similar to that observed in DN hydrogels (Figure 1). Thus, the second loading curve has a much lower initial slope E due to the damage in the lamellar clusters and shows hardening at strain λ above 1.4 because gel deformation becomes homogeneous again. However, heating the damaged gel sample in a water bath at

DOI: 10.1021/acs.macromol.7b00507
Macromolecules 2017, 50, 3647−3654

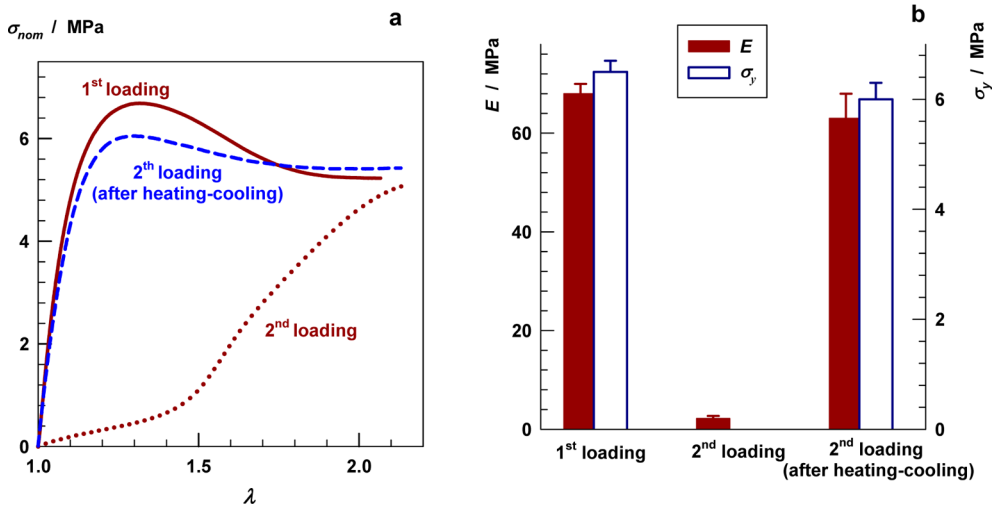

Figure 8. (a) Two successive loading curves up about to 100% elongation for the hydrogel samples with 0.4% C12M. $\dot{\varepsilon} = 8.3 \times 10^{-2}$ s^{-1}. The second loading was conducted without (dotted curve) with heat treatment (dashed curve) of the hydrogel sample by first immersing it in a water bath at 70 °C and then cooling in water to 22 °C. (b) The Young's modulus E and yield stress σ_y of the hydrogel with 0.4% C12M during the first and second loading.

70 °C to melt their crystalline domains and then cooling to 22 °C in water before the second tensile test results in the stress–strain curve shown in Figure 8a by the dashed curve. The gel recovers 93% of both the initial modulus (63 ± 5 MPa) and yield stress (6.0 ± 0.4), indicating that the hydrogels exhibit almost reversible tensile tests (Figure 8b).

The synthetic strategy presented here, based on the use of weak and strong hydrophobes as the minor and major components of the hydrophobic part of the polymer, respectively, can be extended to a variety of hydrophobic and hydrophilic segments. In addition to bulk polymerization described here, solution and micellar polymerization techniques could also be used to prepare high-strength, tough, and stretchable semicrystalline hydrogels.

CONCLUSIONS

Supramolecular semicrystalline hydrogels with a high degree of crystallinity are mechanically strong soft materials exhibiting a Young's modulus of 80–300 MPa and tensile fracture stress of 4–7 MPa. However, they are brittle and rupture at a stretch of less than 20% without yielding. Here, we showed that the incorporation of a small amount of a weak hydrophobe into semicrystalline hydrogels significantly increases their toughness and stretchability without losing their high modulus and high strength. We design a highly entangled physical network based PDMA containing C18A and C12M segments with side chain lengths of 18 and 12 carbons, respectively. By including 0.1–0.4 mol % C12M into the polymer backbone consisting of 70% DMA and 30% C18A segments, we were able to generate more ordered and thinner lamellar crystals with a layered structure. Simultaneously, a brittle-to-ductile transition was observed due to the appearance of necking behavior leading to 10-fold increase of toughness while the modulus and tensile strength remain almost unchanged. The significant toughness improvement upon incorporation of C12M into the semicrystalline hydrogels could be explained with the appearance of active tie molecules interconnecting the lamellar clusters. The hydrogels also exhibit reversible tensile deformation induced by heating above the melting temperature of crystalline domains.

ASSOCIATED CONTENT

Supporting Information

The Supporting Information is available free of charge on the ACS Publications website at DOI: 10.1021/acs.macromol.7b00507.

Experimental details including synthesis, sample preparation, and characterization (PDF)

AUTHOR INFORMATION

Corresponding Author

*(O.O.) E-mail: okayo@itu.edu.tr.

ORCID

Oguz Okay: 0000-0003-2717-4150

Notes

The authors declare no competing financial interest.

ACKNOWLEDGMENTS

Work was supported by the Scientific and Technical Research Council of Turkey (TUBITAK), KBAG 114Z312. O.O. thanks the Turkish Academy of Sciences (TUBA) for partial support.

REFERENCES

(1) Calvert, P. Hydrogels for soft machines. *Adv. Mater.* **2009**, *21*, 743–756.

(2) Tanaka, Y.; Gong, J. P.; Osada, Y. Novel hydrogels with excellent mechanical performance. *Prog. Polym. Sci.* **2005**, *30*, 1–9.

(3) Gong, J. P.; Katsuyama, Y.; Kurokawa, T.; Osada, Y. Double-network hydrogels with extremely high mechanical strength. *Adv. Mater.* **2003**, *15*, 1155–1158.

(4) Tanaka, Y.; Kuwabara, R.; Na, Y.-H.; Kurokawa, T.; Gong, J. P.; Osada, Y. Determination of fracture energy of high strength double network hydrogels. *J. Phys. Chem. B* **2005**, *109*, 11559–11562.

(5) Gong, J. P. Why are double network hydrogels so tough? *Soft Matter* **2010**, *6*, 2583–2590.

(6) Nakajima, T.; Furukawa, H.; Tanaka, Y.; Kurokawa, T.; Osada, Y.; Gong, J. P. True chemical structure of double network hydrogels. *Macromolecules* **2009**, *42*, 2184–2189.

DOI: 10.1021/acs.macromol.7b00507
Macromolecules 2017, 50, 3647–3654

(7) Es-haghi, S. S.; Leonov, A. I.; Weiss, R. A. Deconstructing the double-network hydrogels: The importance of grafted chains for achieving toughness. *Macromolecules* **2014**, *47*, 4769−4777.
(8) Ahmed, S.; Nakajima, T.; Kurokawa, T.; Haque, Md.A.; Gong, J. P. Brittle−ductile transition of double network hydrogels: Mechanical balance of two networks as the key factor. *Polymer* **2014**, *55*, 914−923.
(9) Matsuda, T.; Nakajima, T.; Fukuda, Y.; Hong, W.; Sakai, T.; Kurokawa, T.; Chung, U.; Gong, J. P. Yielding criteria of double network hydrogels. *Macromolecules* **2016**, *49*, 1865−1872.
(10) Es-haghi, S. S.; Leonov, A. I.; Weiss, R. A. On the necking phenomenon in pseudo-semi-interpenetrating double-network hydrogels. *Macromolecules* **2013**, *46*, 6203−6208.
(11) Sun, J.-Y.; Zhao, X.; Illeperuma, W. R. K.; Chaudhuri, O.; Oh, K. H.; Mooney, D. J.; Vlassak, J. J.; Suo, Z. Highly stretchable and tough hydrogels. *Nature* **2012**, *489*, 133−136.
(12) Li, J.; Suo, Z.; Vlassak, J. J. Stiff, strong, and tough hydrogels with good chemical stability. *J. Mater. Chem. B* **2014**, *2*, 6708−6713.
(13) Chen, Q.; Wei, D.; Chen, H.; Zhu, L.; Jiao, C.; Liu, G.; Huang, L.; Yang, J.; Wang, L.; Zheng, J. Simultaneous enhancement of stiffness and toughness in hybrid double network hydrogels via the first, physically linked network. *Macromolecules* **2015**, *48*, 8003−8010.
(14) Sun, T. L.; Kurokawa, T.; Kuroda, S.; Ihsan, A. B.; Akasaki, T.; Sato, K.; Haque, M. A.; Nakajima, T.; Gong, J. P. Physical hydrogels composed of polyampholytes demonstrate high toughness and viscoelasticity. *Nat. Mater.* **2013**, *12*, 932−937.
(15) Hu, X.; Vatankhah-Varnoosfaderani, M.; Zhou, J.; Li, Q.; Sheiko, S. S. Weak hydrogen bonding enables hard, strong, tough, and elastic hydrogels. *Adv. Mater.* **2015**, *27*, 6899−6905.
(16) Matsuda, A.; Sato, J.; Yasunaga, H.; Osada, Y. Order-disorder transition of a hydrogel containing an n-alkyl acrylate. *Macromolecules* **1994**, *27*, 7695−7698.
(17) Tanaka, Y.; Kagami, Y.; Matsuda, A.; Osada, Y. Thermoreversible transition of tensile modulus of hydrogel with ordered aggregates. *Macromolecules* **1995**, *28*, 2574−2576.
(18) Miyazaki, T.; Yamaoka, K.; Gong, J. P.; Osada, Y. Hydrogels with crystalline or liquid crystalline structure. *Macromol. Rapid Commun.* **2002**, *23*, 447−455.
(19) Bilici, C.; Okay, O. Shape memory hydrogels via micellar copolymerization of acrylic acid and n-octadecyl acrylate in aqueous media. *Macromolecules* **2013**, *46*, 3125−3131.
(20) Bilici, C.; Can, V.; Nöchel, U.; Behl, M.; Lendlein, A.; Okay, O. Melt-processable shape-memory hydrogels with self-healing ability of high mechanical strength. *Macromolecules* **2016**, *49*, 7442−7449.
(21) Kurt, B.; Gulyuz, U.; Demir, D. D.; Okay, O. High-strength semi-crystalline hydrogels with self-healing and shape memory functions. *Eur. Polym. J.* **2016**, *81*, 12−23.
(22) Uemura, Y.; McNulty, J.; Macdonald, P. M. Associative behavior and diffusion coefficients of hydrophobically modified poly(N,N-dimethylacrylamides). *Macromolecules* **1995**, *28*, 4150−4158.
(23) Peppas, N. A. *Hydrogels in Medicine and Pharmacy*; Wiley: New York, 1987.
(24) Relogio, P.; Martinho, J. M. G.; Farinha, J. P. S. Effect of surfactant on the intra- and intermolecular association of hydrophobically modified poly(N,N-dimethylacrylamide). *Macromolecules* **2005**, *38*, 10799−10811.
(25) Hempel, E.; Budde, H.; Höring, S.; Beiner, M. On the crystallization behavior of frustrated alkyl groups in poly(n-octadecyl methacrylate). *J. Non-Cryst. Solids* **2006**, *352*, 5013−5020.
(26) Hiller, S.; Pascui, O.; Budde, H.; Kabisch, O.; Reichert, D.; Beiner, M. Nanophase separation in side chain polymers: new evidence from structure and dynamics. *New J. Phys.* **2004**, *6*, 10.
(27) Tuncaboylu, D. C.; Argun, A.; Sahin, M.; Sari, M.; Okay, O. Structure optimization of self-healing hydrogels formed via hydrophobic interactions. *Polymer* **2012**, *53*, 5513−5522.
(28) Tuncaboylu, D. C.; Sahin, M.; Argun, A.; Oppermann, W.; Okay, O. Dynamics and large strain behavior of self-healing hydrogels with and without surfactants. *Macromolecules* **2012**, *45*, 1991−2000.
(29) Uchida, M.; Kurosawa, M.; Osada, Y. Swelling process and order-disorder transition of hydrogel containing hydrophobic ionizable groups. *Macromolecules* **1995**, *28*, 4583−4586.
(30) Miyazaki, T.; Kaneko, T.; Gong, J. P.; Osada, Y. Effects of carboxyls attached at alkyl side chain ends on the lamellar structure of hydrogels. *Macromolecules* **2001**, *34*, 6024−6028.
(31) Alig, I.; Jarek, M.; Hellmann, G. P. Restricted segmental mobility in side-chain crystalline comblike polymers studied by dielectric relaxation measurements. *Macromolecules* **1998**, *31*, 2245−2251.
(32) Floudas, G.; Stepánek, P. Structure and dynamics of poly(n-decyl methacrylate) below and above the glass transition. *Macromolecules* **1998**, *31*, 6951−6957.
(33) Plate, N. A.; Shibaev, V. P. Comb-like polymers. Structure and properties. *Macromol. Rev.* **1974**, *8*, 117−253.
(34) Miller, R. L.; Boyer, R. F.; Heijboer, J. X-ray scattering from amorphous acrylate and methacrylate polymers: Evidence of local order. *J. Polym. Sci., Polym. Phys. Ed.* **1984**, *22*, 2021−2041.
(35) Shang, S.; Huang, S. J.; Weiss, R. A. Synthesis and characterization of itaconic anhydride and stearyl methacrylate copolymers. *Polymer* **2009**, *50*, 3119−3127.
(36) The length of a fully extended hydrocarbon chain l_{max} (in nm) was estimated by $l_{max} = 0.15 + 0.1265n_c$, where n_c is the number of carbon atoms in the chain.[37]
(37) Stokes, R. J.; Evans, D. F. *Fundamentals of Interfacial Engineering*; Wiley-VCH: 1997; p 215.
(38) Kauzmann, W.; Eyring, H. The viscous flow of large molecules. *J. Am. Chem. Soc.* **1940**, *62*, 3113−3125.
(39) Ward, I. M.; Hadley, D. N. *Mechanical Properties of Solid Polymers*; Wiley: Chichester, UK, 2000.
(40) McCrum, N. G.; Buckley, C. P.; Bucknall, C. B. *Principles of Polymer Engineering*; Oxford University Press: New York, 1997.
(41) Annable, T.; Buscall, R.; Ettelaie, R.; Whittlestone, D. The rheology of solutions of associating polymers: Comparison of experimental behavior with transient network theory. *J. Rheol.* **1993**, *37*, 695−726.
(42) Tripathi, A.; Tam, K. C.; McKinley, G. H. Rheology and dynamics of associative polymers in shear and extension: Theory and experiments. *Macromolecules* **2006**, *39*, 1981−1999.
(43) In ref 21, the activation energy of semicrystalline hydrogels was estimated using eq 1 by neglecting the pre-exponential factor ε_0. This is inaccurate as the factor ε_0 is much larger than $\dot{\varepsilon}$.
(44) Guo, H.; Zhang, Y.; Xue, F.; Cai, Z.; Shang, Y.; Li, J.; Chen, Y.; Wu, Z.; Jiang, S. In-situ synchrotron SAXS and WAXS investigations on deformation and $\alpha-\beta$ transformation of uniaxial stretched poly(vinylidene fluoride). *CrystEngComm* **2013**, *15*, 1597−1606.
(45) Spitalsky, Z.; Bleha, T.; Cifra, P. Energy elasticity of tie molecules in semicrystalline polymers. *Macromol. Theory Simul.* **2002**, *11*, 513−524.
(46) Humbert, S.; Lame, O.; Chenal, J.-M.; Rochas, C.; Vigier, G. Small strain behavior of polyethylene: In situ SAXS measurements. *J. Polym. Sci., Part B: Polym. Phys.* **2010**, *48*, 1535−1542.
(47) Nitta, K.-H.; Takayanagi, M. Novel proposal of lamellar clustering process for elucidation of tensile yield behavior of linear polyethylenes. *J. Macromol. Sci., Part B: Phys.* **2003**, *42*, 107−126.
(48) Nitta, K.-H.; Takayanagi, M. Role of tie molecules in the yielding deformation of isotactic polypropylene. *J. Polym. Sci., Part B: Polym. Phys.* **1999**, *37*, 357−368.
(49) Nitta, K.-H.; Takayanagi, M. Tensile yield of isotactic polypropylene in terms of a lamellar-cluster model. *J. Polym. Sci., Part B: Polym. Phys.* **2000**, *38*, 1037−1044.
(50) Gao, R.; Kuriyagawa, M.; Nitta, K.-H.; He, X.; Liu, B. Structural interpretation of Eyring activation parameters for tensile yielding behavior of isotactic polypropylene solids. *J. Macromol. Sci., Part B: Phys.* **2015**, *54*, 1196−1210.

DOI: 10.1021/acs.macromol.7b00507
Macromolecules 2017, 50, 3647−3654